Cell Host & Microbe
Article

The Interferon-Inducible Protein Viperin Inhibits Influenza Virus Release by Perturbing Lipid Rafts

Xiuyan Wang,[1] Ella R. Hinson,[1] and Peter Cresswell[1,2,*]
[1] Department of Immunobiology
[2] Howard Hughes Medical Institute
Yale University School of Medicine, 300 Cedar Street, New Haven, CT 06520-8011, USA
*Correspondence: peter.cresswell@yale.edu
DOI 10.1016/j.chom.2007.06.009

SUMMARY

Interferons initiate the host antiviral response by inducing a number of genes, most with no defined antiviral function. Here we show that the interferon-induced protein viperin inhibits influenza A virus release from the plasma membrane of infected cells. Viperin expression altered plasma membrane fluidity by affecting the formation of lipid rafts, which are detergent-resistant membrane microdomains known to be the sites of influenza virus budding. Intracellular interaction of viperin with farnesyl diphosphate synthase (FPPS), an enzyme essential for isoprenoid biosynthesis, decreased the activity of the enzyme. Overexpression of FPPS reversed viperin-mediated inhibition of virus production and restored normal membrane fluidity, and reduction of FPPS levels by siRNA inhibited virus release and replication, indicating that the FPPS interaction underlies viperin's effects. These findings suggest that targeting the release stage of the life cycle may affect the replication of many enveloped viruses. Furthermore, FPPS may be an attractive target for antiviral therapy.

INTRODUCTION

Interferons (IFNs) represent the first line of defense against viral infection. Hundreds of genes are regulated by IFN (Samuel, 2001), and their products are the mediators of the host antiviral response. Many steps in the viral replication cycle are potential targets of IFN-inducible proteins. PKR, which binds double-stranded (ds) RNA, phosphorylates eIF2α and blocks de novo protein synthesis (Clemens and Elia, 1997). 2′-5′ oligoadenylate synthase (OAS), another dsRNA-binding protein, catalyzes the synthesis of 2′-5′ oligoadenylates (Kerr and Brown, 1978) and activates the latent endoribonuclease RNaseL, which then degrades single-stranded RNAs and halts viral replication (Player and Torrence, 1998). The Mx GTPase disrupts the nuclear replication phase of RNA viruses (Kochs and Haller, 1999a, 1999b). ISG15 blocks ubiquitination of Gag and Tsg101 and subsequently inhibits the release of HIV (Okumura et al., 2006). However, the mechanisms of action of the vast majority of IFN-inducible proteins remain unexplored.

Viperin is an evolutionarily conserved protein that is highly inducible by both type I and type II IFNs (Chin and Cresswell, 2001). It has been identified in organisms as diverse as fish (Boudinot et al., 2000; Sun and Nie, 2004), rodents (Grewal et al., 2000), and primates (Chin and Cresswell, 2001; Zhu et al., 1997). Infection by many viruses strongly induces viperin expression (Boudinot et al., 2000; Chin and Cresswell, 2001; Helbig et al., 2005; Khaiboullina et al., 2005; Zhu et al., 1997), suggesting a role in the host antiviral response. Moreover, we previously showed that pre-expression of viperin in human fibroblasts significantly inhibits the replication of human cytomegalovirus (hCMV) (Chin and Cresswell, 2001). Recently, viperin has also been shown to be important for the host anti-HIV responses (Rivieccio et al., 2006).

In this study, we demonstrate that expression of viperin inhibits influenza virus replication by perturbing its release from the plasma membrane. Influenza virus buds from lipid rafts, and we find that viperin expression disrupts the plasma membrane by perturbing lipid rafts in a manner dependent on the ability of viperin to bind and inhibit FPPS, an enzyme involved in the synthesis of multiple isoprenoid-derived lipids. Strikingly, viperin does not affect the replication of vesicular stomatitis virus (VSV), which also buds from the plasma membrane but does not require lipid rafts to do so.

RESULTS

Establishing a Viperin-Inducible Cell System

Pathogens such as viruses, and virus-derived pathogen-associated molecular patterns such as dsRNA, are potent IFN inducers. After secretion, IFN binds to its receptor and activates the JAK-STAT pathway, which induces the expression of responsive genes, including viperin (Figure 1A). To facilitate the analysis of the antiviral mechanism of viperin, we generated a stable HeLa Tet-on-derived cell line in which mouse viperin can be specifically induced by doxycycline and the level of expression regulated by varying the doxycycline concentration (Figure 1B and

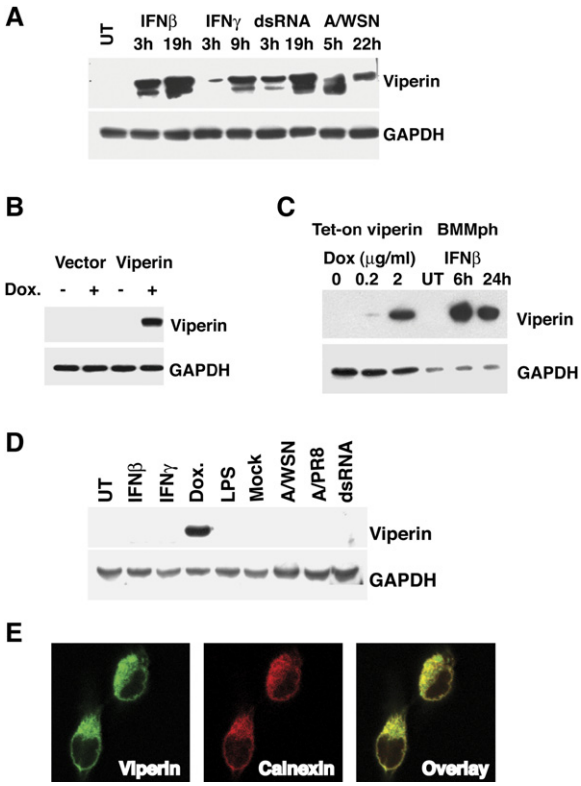

Figure 1. Establishment of HeLa Tet-on Viperin-Inducible Cells

(A) Expression of viperin in mouse macrophages. Primary mouse macrophages were treated with 200 U/ml IFNβ, 200 U/ml IFNγ, or 40 μg/ml dsRNA or infected with influenza A/WSN virus at an moi of 3.

(B) Expression of mouse viperin in HeLa Tet-on viperin-inducible cells. HeLa Tet-on vector-alone cells or HeLa Tet-on viperin-inducible cells were untreated (–) or treated (+) with 2 μg/ml doxycycline for 16 hr.

(C) Levels of viperin expression in HeLa Tet-on viperin-inducible cells and bone marrow-derived macrophages (BMMph). HeLa Tet-on viperin cells were either untreated or treated with 0.2 μg/ml or 2 μg/ml doxycycline for 24 hr. BMMph were either untreated or treated with 500 U/ml IFNβ for 6 hr or 24 hr. Twenty micrograms of total cell lysates were loaded.

(D) HeLa Tet-on cells do not express endogenous human viperin. HeLa Tet-on viperin-inducible cells were treated with 500 U/ml IFNβ, 500 U/ml IFNγ, 2 μg/ml doxycycline, 1 μg/ml LPS, or 50 μg/ml dsRNA, or mock infected or infected with influenza A/WSN or A/PR8 at an moi of 3. Cell lysates from (A)–(D) were subjected to SDS-PAGE and western blot analysis using an antiserum recognizing both human and mouse viperin. GAPDH was used as a loading control.

(E) Viperin localizes to the ER in viperin-inducible cells. The cells were treated with doxycycline for 24 hr and stained with a mouse monoclonal anti-viperin antibody and a rabbit antiserum to calnexin, followed by Alexa 488-conjugated goat anti-mouse Ig and Alexa 546-conjuated goat anti-rabbit Ig secondary antisera. Images were acquired using a Leica TCS SP2 confocal microscope.

Figure 1C). In the experiments reported, we used doxycycline at 2 μg/ml because the level of expression at this concentration is comparable to the endogenous viperin level induced by IFN-β treatment of bone marrow-derived macrophages (BMMph) (Figure 1C). Doxycycline-induced viperin colocalized with the endoplasmic reticulum (ER) marker calnexin (Figure 1E), which is consistent with the normal intracellular distribution of human viperin (Chin and Cresswell, 2001). Endogenous human viperin was not detectable in this cell line after treatment with IFN, LPS, dsRNA, or influenza A virus infection (Figure 1D). This is consistent with earlier observations for HeLa cells (Chin and Cresswell, 2001), and it avoids potential experimental complications caused by endogenous viperin expression.

Viperin Expression Inhibits Influenza Virus Replication by Blocking Viral Release from the Plasma Membrane

We previously showed that expression of viperin affected the replication of hCMV. The complexity of the hCMV replication cycle, however, has hindered analysis of the mechanism. We therefore elected to use influenza A, a negative-stranded RNA virus, as a model virus. Viperin was strongly induced in primary mouse macrophages by influenza A/WSN virus infection (Figure 1A), and a similar response was observed upon infection of mouse embryonic fibroblasts (data not shown), suggesting that viperin may play a role in the host anti-influenza response.

To determine whether viperin expression could inhibit influenza A/WSN virus replication, viperin-inducible cells or vector control cells were overnight pretreated with doxycycline or left untreated, and then infected with A/WSN virus at a multiplicity of infection (moi) of 0.02. Virus replication was substantially inhibited by the expression of viperin. At 48 hr postinfection, approximately 10^7 plaque-forming units (PFU)/ml were obtained from control cells, whether or not they were treated with doxycycline, or from untreated viperin-inducible cells (Figure 2A). In contrast, only 10^4 PFU/ml were obtained from doxycycline-treated viperin-inducible cells (Figure 2A). Influenza A/WSN replication was consistently inhibited upon doxycycline treatment of multiple viperin-inducible clones (data not shown).

To investigate the antiviral mechanism, we first wished to determine the step of the viral replication cycle targeted by viperin. A productive infection by influenza A virus begins when it binds to its cell surface receptor, sialic acid. The bound virus is subsequently internalized by endocytosis, and the acidic endosomal pH triggers membrane fusion, releasing the viral genome into the cytosol and ultimately the nucleus, where viral mRNA synthesis and genome replication occur. Viral mRNAs enter the cytosol and initiate viral protein synthesis. The viral transmembrane glycoproteins, hemagglutinin (HA) and neuraminidase (NA), traffic to lipid rafts in the plasma membrane where viral budding takes place (Leser and Lamb, 2005; Scheiffele et al., 1999). The matrix protein (M1), nuclear export protein (NEP), and the nucleoprotein (NP) move to the nucleus where, with assistance from cellular factors, they form the nucleocapsid. The nucleocapsid translocates the viral genome to the cytosol and finally to the plasma membrane. Here the viral replication cycle culminates in the assembly and release of progeny virions (Lamb and Krug, 2001). No significant effects of viperin

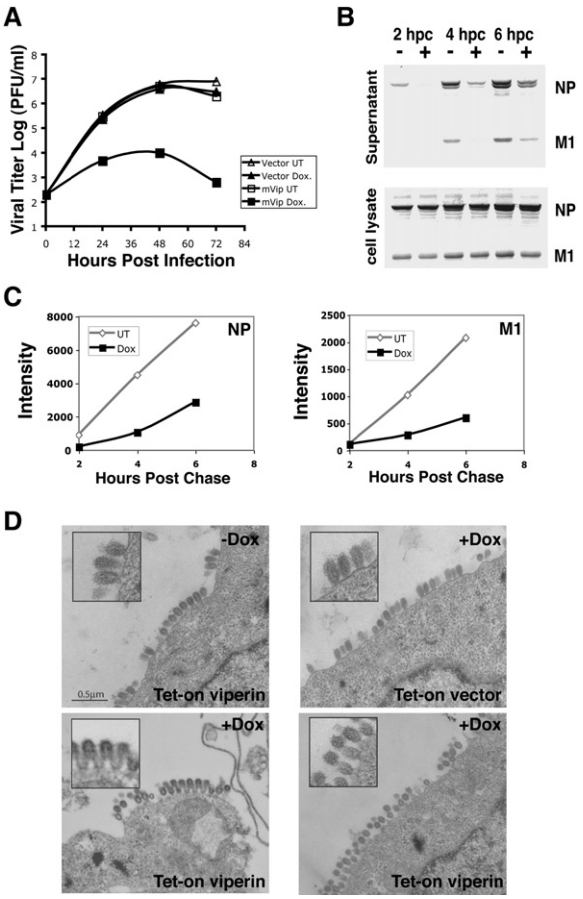

Figure 2. Viperin Expression Inhibits Influenza A Virus Replication and Release

(A) Expression of viperin inhibits influenza A/WSN virus replication. Control cells or viperin-inducible cells were untreated or treated with doxycycline for 16 hr and infected with influenza A/WSN virus at an moi of 0.02. Viral titers were determined at 24, 48, and 72 hr postinfection by plaque assay.

(B) Expression of viperin inhibits influenza A/WSN virus release. Viperin-inducible cells were untreated (−) or pretreated (+) with doxycycline for 24 hr and infected with influenza A/WSN virus at an moi of 3. After 16 hr, cells were labeled with ^{35}S-methionine and cysteine for 20 min and chased for 2, 4, and 6 hr. Viral proteins released in the supernatant and in cell extracts were immunoprecipitated using a goat anti-influenza virus antiserum and subjected to SDS-PAGE and autoradiography.

(C) Quantitation of released NP and M1 in (B).

(D) Expression of viperin inhibits influenza A virus budding. Control or viperin-inducible cells, untreated or pretreated with doxycycline, were infected with influenza A/WSN virus for 14 hr and subjected to thin-section EM.

expression were observed on the early stages of replication, including receptor binding (Figure S1A in the Supplemental Data available with this article online), viral genome replication (data not shown), protein synthesis, protein stability (Figure S1B), and protein localization (Figure S1C). However, viral release was severely inhibited by viperin expression. Doxycycline treatment of the inducible cells led to an 80% reduction in released virus compared to control cells, measured by immunoprecipitation of detergent-treated supernatants and SDS-PAGE (Figure 2B, upper panel; Figure 2C). The intracellular levels of NP and M1 proteins were unaffected (Figure 2B, lower panel).

To characterize more fully the viral release defect, infected cells were examined by thin-section electron microscopy. In untreated viperin-inducible cells or doxycycline-treated control cells (Figure 2D, upper panels), the membranes of the progeny virions still attached to the cell membrane appeared ready for pinching off and release. In contrast, many of the virions on the surface of viperin-expressing cells displayed either an abnormal elongated stalk-like phenotype or a "daisy-chain" structure in which two or more viral particles appear to be linked by a connecting membrane (Figure 2D, lower panels). The images suggest that initial bud formation occurs in viperin-expressing cells, but the release of progeny virions is inhibited. Initiation of assembly of a second virus at a budding site where a virion is arrested may lead to the "daisy-chain" structure. An analysis of 188 budding events in viperin-expressing cells showed that 43% of them displayed either the elongated stalk or "daisy chain" phenotypes, while in non-viperin-expressing infected cells only 3.6% were abnormal. A similar "daisy-chain" budding defect has been observed in influenza A viruses with mutations in the cytoplasmic tail of NA (Barman et al., 2004), or truncation in the M2 protein (McCown and Pekosz, 2006). Similar structures have also been observed in cells infected with HIV late domain mutants (Garrus et al., 2001).

Expression of Viperin Disrupts Lipid Rafts

Influenza virions bud from lipid raft microdomains on the plasma membrane (Leser and Lamb, 2005; Scheiffele et al., 1999). We hypothesized that the budding defect we observed in viperin-expressing cells may be due to a disturbance of lipid-raft microdomains on the plasma membrane. One characteristic of lipid rafts is the poor extraction of raft-associated proteins, such as influenza virus HA, by nonionic detergents at 4°C (Scheiffele et al., 1997). If viperin expression disrupts lipid raft formation, we would expect to see an increase in the extraction of HA molecules from viperin-expressing cells in the nonionic detergent Triton X-100. Consistent with this hypothesis, HA was more readily extracted from viperin-expressing cells by a low concentration of Triton X-100 at 4°C (Figure 3A, left panel). The detergent solubility of vesicular stomatitis virus-glycoprotein (VSV-G), which does not associate with lipid rafts (Scheiffele et al., 1999), was the same in the presence or absence of viperin, as were the nonmembrane proteins influenza NP (Figure 3A, left panel) and VSV nucleoprotein (N) (Figure 3A, right panel). Lipid raft microdomains are highly enriched in sphingolipids, and staining of the sphingolipid GM1 by the cholera toxin B subunit has been used to detect them. Lipid raft-associated proteins, such as the GPI-anchored protein placental alkaline phosphatase (PLAP), cluster with cholera toxin-crosslinked GM1 after antibody-induced patching, and the copatching of lipid-raft associated proteins is significantly reduced

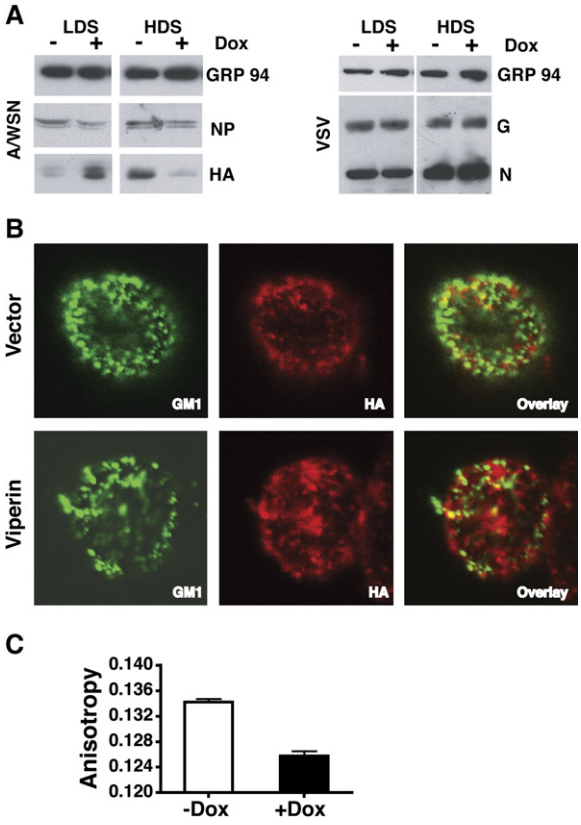

Figure 3. Viperin Expression Disrupts Lipid Rafts

(A) Viperin expression enhances extraction of HA by Triton X-100. Viperin-inducible cells, untreated or treated with doxycycline for 24 hr, were infected with A/WSN virus for 18 hr or with VSV virus for 5 hr at an moi of 5. Cells were then extracted with 0.1% Triton X-100 at 4°C for 30 min. After centrifugation, the supernatant (LDS, *l*ow-concentration *d*etergent-sensitive) was removed, and the pelleted cells were further extracted with 1% Triton X-100 (HDS, *h*igh-concentration *d*etergent-sensitive). The LDS and HDS extracts were subjected to SDS-PAGE and western blot analysis using antibodies specific for HA, NP, VSV-N, and VSV-G proteins. GRP94 was used as a loading control.

(B) Viperin expression disrupts copatching of HA and GM1. HeLa Tet-on cells were transiently transfected with HA plus vector or with HA plus viperin expression plasmids. Forty-eight hours posttransfection, Alexa 488-conjugated cholera toxin B subunit was used to induce GM1 patching at room temperature. Patching of HA was induced using a monoclonal antibody against HA followed by Alexa 633-conjugated goat anti-mouse IgG secondary antibody. Cells were fixed and images acquired using a Leica TCS SP2 confocal microscope. Digital Alexa 633 images were pseudocolored red for better visualization. Copatching of HA and GM1 was largely disrupted in the viperin-expressing cells.

(C) Membrane fluidity in viperin-nonexpressing (−Dox) and viperin-expressing (+Dox) cells. HeLa Tet-on RFP-viperin cells were either untreated or pretreated with doxycycline for 24 hr. Cells were labeled with DPH, and fluorescent anisotropy was measured.

after lipid raft disruption by cholesterol depletion (Harder et al., 1998). We therefore asked whether expression of viperin could disrupt the coclustering of HA or PLAP induced by specific antibodies and GM1 induced by cholera toxin. We found that both HA and PLAP copatched with GM1 in control cells as previously observed (Harder et al., 1998), but the copatching was largely disrupted by viperin expression (Figure 3B and Figure S2). This suggests that viperin expression indeed disrupts lipid raft microdomains.

Previous studies have shown that IFN treatment can induce an increase in membrane fluidity and in the lateral diffusion coefficients of certain membrane proteins (Balint et al., 2005; Nathan et al., 1998). To directly monitor whether viperin expression leads to a change in membrane fluidity, we measured the membrane anisotropy using 1,6-diphenyl-1,3,5-hexatriene (DPH) as a probe. We found a significantly lower anisotropy in doxycycline-induced viperin-expressing cells compared to untreated viperin-nonexpressing cells (Figure 3C), reflecting a lower membrane microviscosity and an increase in membrane fluidity. This effect was not due to doxycycline treatment, because no significant change of membrane anisotropy was found in the vector alone cells in the presence or absence of doxycycline (Figure S3). The cumulative data strongly argue that viperin expression affects lipid raft formation.

Lipid rafts are tightly packed, liquid-ordered microdomains enriched in sphingolipids and cholesterol. Their rigid structure results in decreased lateral diffusion of the membrane proteins in lipid rafts compared to those in liquid-disordered nonraft regions (Shvartsman et al., 2003). We therefore hypothesized that surface HA molecules in viperin-expressing cells would exhibit increased mobility compared to nonexpressing cells. To test this, we used the technique of fluorescence recovery after photobleaching (FRAP). To facilitate the analysis, we generated an inducible HeLa-derived cell line expressing a red fluorescent protein (RFP)-viperin chimera. RFP-viperin was induced by doxycycline treatment (Figure 4A) and, like wild-type viperin, it colocalized with calnexin (Figure S4) and inhibited the replication of influenza A/WSN virus (Figure 4B). RFP-viperin-inducible cells were either treated with doxycycline, or left untreated, for 24 hr and then infected with influenza A virus for 14 hr. Cell surface HA was labeled with an Alexa 488-conjugated Fab fragment of the HA-specific monoclonal antibody H17-L2 (Arnon et al., 2001) at 4°C, and FRAP analysis was conducted at 22°C. Typical surface staining and fluorescent recovery curves of HA expressed on the surface of viperin-expressing and nonexpressing cells are shown in Figure 4C. Consistent with our hypothesis, viperin expression increased the lateral diffusion rate of HA. The half-life of fluorescence recovery (T1/2) was significantly reduced in viperin-expressing cells compared to control cells (T1/2 of 33.2 s versus T1/2 of 59.0 s; Figure 4D, upper panel). Viperin expression increased the lateral diffusion coefficient of HA by a factor of 2, which is consistent with a change of an ordered lipid phase to a disordered lipid phase (Almeida et al., 1993). The rate of fluorescence recovery for VSV-G, a transmembrane glycoprotein that is not raft associated, was unchanged by viperin expression (T1/2 of 26.5 s versus T1/2 of 26.4 s; Figure 4D, lower panel).

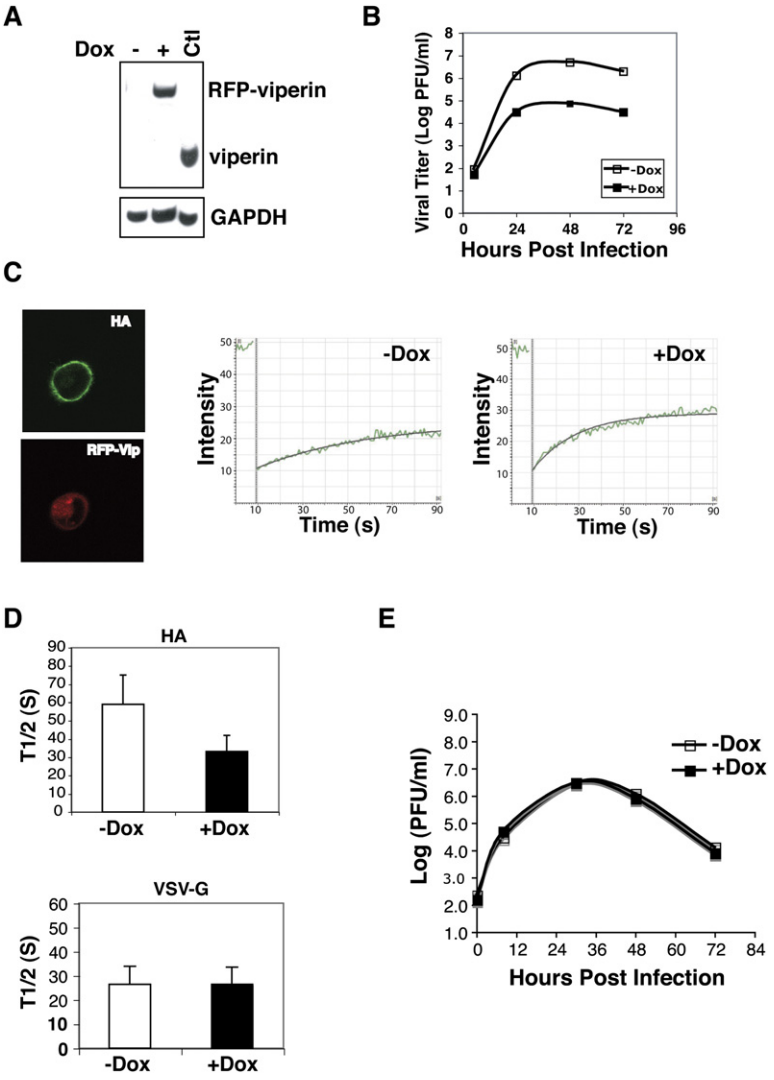

Figure 4. Viperin Expression Affects the Lateral Mobility of Influenza HA

(A) Expression of RFP-viperin in HeLa Tet-on viperin-inducible cells. The RFP-viperin-inducible cells were untreated (−) or treated (+) with 2 μg/ml doxycycline for 16 hr. Cell lysates were subjected to Western blot analysis using an antiserum recognizing both human and mouse viperin. Cell lysates of doxycycline-treated HeLa Tet-on cells expressing untagged viperin were used as a control (Ctl). GAPDH was used as a loading control.

(B) RFP-viperin antiviral activity for influenza A/WSN virus. RFP-viperin-inducible cells were untreated or treated with doxycycline, infected, and supernatants were subjected to a plaque assay as in Figure 2A.

(C) Staining of surface HA by monovalent Alexa 488-conjugated H17-L2 Fab, the expression of RFP-viperin, and a representative FRAP curve in RFP-viperin-expressing (+Dox) or nonexpressing (−Dox) cells.

(D) Fluorescence recovery half-lives of influenza HA and VSV-G-GFP molecules. For HA, cells were either untreated (−Dox) or treated with doxycycline (+Dox) for 24 hr and infected with influenza A/WSN virus for 14 hr at an moi of 3. Cells were stained with Alexa 488-conjugated H17-L2 Fab on ice for 30 min. A minimum of 12 cells in each category were subjected to FRAP analysis. Statistical significance (***$p < 0.001$ for −Dox versus +Dox cells) by Student's t test. For VSV-G, RFP-viperin-inducible cells were transfected with VSV-G-GFP expression plasmid for 24 hr. Cells were then either untreated (−Dox) or treated with doxycycline (+Dox) for another 24 hr. Thirty-three −Dox and 29 +Dox cells were subjected to FRAP analysis. Statistical significance ($p = 0.97$ for −Dox versus +Dox cells) was determined by Student's t test.

(E) Expression of viperin does not inhibit VSV replication. HeLa Tet-on viperin-inducible cells were untreated or treated with doxycycline for 16 hr and infected with VSV at an moi of 0.001. Viral titers were determined at 0, 8, 30, 48, and 72 hr postinfection by plaque assay.

Significantly, the replication of VSV, which does not involve lipid rafts, was not affected by the expression of viperin (Figure 4E). These observations further support the hypothesis that viperin expression inhibits the release of influenza virus by disrupting lipid rafts.

Viperin Interacts with and Inhibits Farnesyl Diphosphate Synthase

To investigate further the antiviral mechanism, we looked for viperin-interacting proteins using yeast two-hybrid screening. A cDNA corresponding to farnesyl diphosphate synthase (FPPS) was isolated. FPPS is a key enzyme in the isoprenoid biosynthetic pathway: it catalyzes the sequential condensation of dimethylallyl pyrophosphate with two molecules of isopentenyl diphospate to form farnesyl pyrophosphate (FPP). FPP is a biosynthetic precursor of cholesterol, farnesylated and geranylated proteins, ubiquinones, dolichols and heme a (Szkopinska and Plochocka, 2005). We confirmed that endogenous FPPS and viperin interacted in vivo in IFN-treated mouse RAW264.1 cells by coimmunoprecipitation (Figure 5A). We also found that viperin expression in HeLa Tet-on cells led to a reduction in FPPS enzymatic activity, by 20% after 24 hr and 50% after 48 hr of doxycycline treatment (Figure 5B).

Overexpression of FPPS Reverses the Viperin Effects

Because FPPS is a pivotal enzyme involved in lipid metabolism, and viperin inhibited its activity, we tested whether overexpression of FPPS could reverse the increased lateral mobility of plasma membrane HA molecules induced

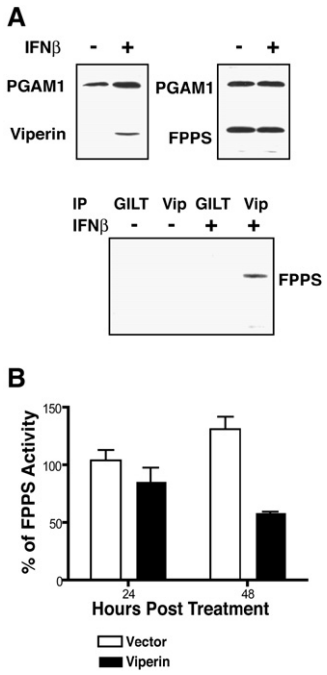

Figure 5. Viperin Interacts with FPPS and Inhibits Its Activity

(A) Endogenous viperin interacts with FPPS. RAW264.1 cells were either untreated (−) or treated (+) with IFN-β for 16 hr. Expression of viperin and FPPS were determined by western blotting (upper panels). Phosphoglycerate mutase 1 (PGAM1) was used as a loading control. Cell lysates were also immunoprecipitated with mouse anti-viperin mAb. A mouse mAb to mouse GILT, a protein highly expressed in RAW264.1 cells, was used as a control. Immune complexes were separated by SDS-PAGE, and FPPS was detected by western blotting (lower panel).

(B) The activity of FPPS is reduced by viperin expression. Control and viperin-inducible cells were either untreated or treated with doxycycline for 24 hr and 48 hr. FPPS activity was determined by synthesis of ^{14}C-FPP from geranyl pyrophosphate and ^{14}C-isopentenyl pyrophosphate. The values in doxycycline-treated cells were normalized to their untreated counterparts.

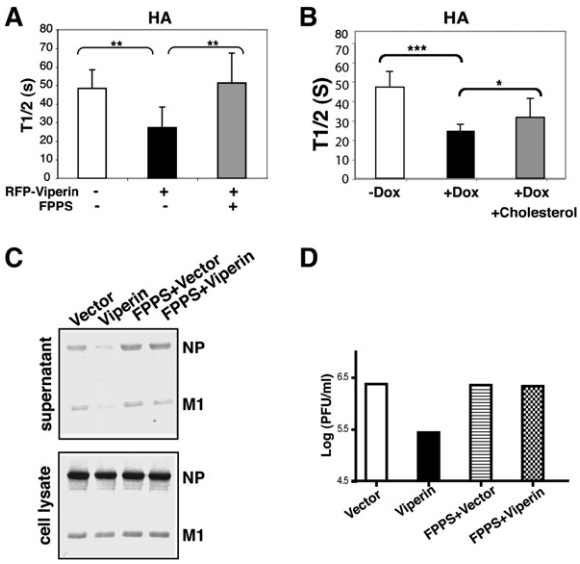

Figure 6. Overexpression of FPPS Reverses the Antiviral Activity of Viperin

(A) Expression of FPPS in viperin-expressing cells restores the normal lateral diffusion rate of HA. HeLa Tet-on cells were transiently transfected with combinations of vectors encoding RFP-viperin or FPPS for 24 hr, infected with influenza A/WSN virus, subjected to FRAP analysis as described in Figure 4D, and the half-lives of recovery were calculated. For nontransfected cells versus RFP-viperin-transfected cells, $^{**}p < 0.01$; for nontransfected cells versus RFP-viperin- and FPPS-cotransfected cells, $p > 0.05$; for RFP-viperin-transfected versus RFP-viperin- and FPPS-cotransfected cells, $^{**}p < 0.01$.

(B) In vitro loading of cholesterol partially restores the normal fluorescence recovery half-lives of influenza HA. For HA, cells were either untreated (−Dox), treated with doxycycline (+Dox), or treated with a combination of doxycycline and cholesterol (+Dox +Cholesterol) for 24 hr and infected with influenza A/WSN virus for 14 hr at an moi of 3. FRAP analysis was conducted as in (A), and a minimum of 27 cells in each category were subjected to FRAP analysis. Statistical significance ($^{***}p < 0.001$ for −Dox versus +Dox; $^{*}p < 0.05$ for +Dox versus +Dox+Cholesterol, and $p > 0.05$ for −Dox versus +Dox+Cholesterol) was determined by the one-way ANOVA method.

(C) FPPS expression restores viral release in viperin-expressing cells. HeLa Tet-on cells were transiently transfected with vector, viperin, FPPS, or viperin plus FPPS expression plasmids. After 24 hr, cells were infected with influenza A/WSN virus for 16 hr, pulse-labeled with ^{35}S-methionine and cysteine for 20 min, and chased for 2 hr. Supernatants and cell lysates were immunoprecipitated and subjected to SDS-PAGE and autoradiography as in Figure 2B.

(D) FPPS abrogates the viperin-mediated inhibition of influenza A/WSN virus replication. HeLa Tet-on cells transiently transfected as in (C) were infected with influenza A/WSN virus at an moi of 0.02. Virus titers in the supernatant were determined by plaque assay 24 hr postinfection. One of two representative experiments is shown.

by viperin. HeLa Tet-on cells were transfected with vector alone, RFP-viperin expression plasmid plus the vector, or a mixture of the RFP-viperin and FPPS expression plasmids. At 24 hr posttransfection, the cells were infected with influenza A/WSN virus at an moi of 3. Cell surface HA was labeled with fluorescent anti-HA Fab 14 hr postinfection, and FRAP analysis was conducted. As we observed in the RFP-viperin-inducible cells, transiently expressed RFP-viperin significantly increased the lateral mobility of HA compared to control cells (recovery T1/2 of 27.2 s versus 48.2 s; Figure 6A). Importantly, coexpression of FPPS reversed the viperin effect, increasing the T1/2 for recovery to 51.2 s (Figure 6A). In addition, we found that in vitro loading of exogenous cholesterol, one of the downstream products of FPPS, into viperin-expressing cells significantly decreased the lateral mobility of HA (recovery T1/2 of 35.7 s versus T1/2 of 23.8 s, Figure 6B). These data suggest that the enhanced membrane fluidity upon viperin expression is caused by its inhibition of FPPS activity, and that cholesterol metabolism might be a factor contributing to the effect. Since FPPS catalyzes the biosynthesis of FPP, a precursor for protein isoprenylation, we also tested whether the inhibition of FPPS by viperin affected isoprenylation of the cellular proteins Cdc42 (Figure S5), Rab5, and RhoB (data not shown). Treatment of the cells with lovastatin, an inhibitor of HMG reductase, which acts upstream of FPPS in the biosynthetic pathway,

led to decreased isoprenylation of these proteins and therefore reduced partitioning into Triton X-114 detergent fractions. However, no such inhibition was detected in viperin-expressing cells (Figure S5). This argues that the antiviral activity of viperin is not likely to be mediated by a general reduction in protein isoprenylation.

We next examined whether overexpression of FPPS in viperin-expressing cells could restore influenza virus production. HeLa Tet-on cells transiently transfected with plasmids encoding viperin or FPPS cDNA, or with a combination of the two, were infected with influenza A/WSN virus. The cells were pulse labeled with ^{35}S-methionine and chased, and virus release into the supernatant was assessed. Consistent with the results obtained with the inducible cells (Figure 2B), transiently expressed viperin inhibited viral release (Figure 6C). Importantly, coexpression of FPPS largely reversed the inhibition (Figure 6C). Viral titers in the transiently transfected cells were also determined at 24 hr postinfection, and coexpression of FPPS consistently reversed the observed viperin-induced decrease in virus production (Figure 6D).

Reduction of FPPS Expression by siRNA Inhibits Influenza Replication and Release

To further study the functional significance of FPPS in the viral replication cycle, we used specific siRNA oligonucleotides to efficiently reduce cellular FPPS levels (Figure 7A). Inhibition of FPPS expression led to a decrease in the viral titer produced by infected cells of approximately 10-fold (Figure 7B). Consistent with the effects seen in viperin-expressing cells (Figure 2B), knocking down FPPS also inhibited viral release measured directly by metabolic labeling and immunoprecipitation. Quantitation of the SDS-PAGE bands indicated that the amounts of viral protein released by the infected cells were reduced by approximately 50% (Figure 7C). These observations suggest that the viperin-induced inhibition of influenza virus release is at least partially mediated by its ability to bind and inhibit FPPS.

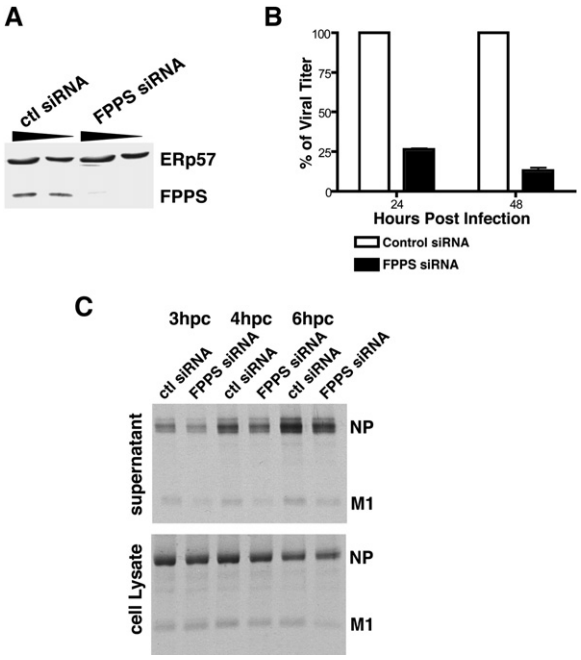

Figure 7. FPPS Plays an Important Role in Influenza A Viral Replication and Release

(A) Specific knockdown of FPPS by siRNA. HeLa cells were transfected twice with either control or FPPS-specific siRNA oligonucleotides at 24 hr intervals. Cell lysates were made 24 hr after the second transfection, subjected to SDS-PAGE, and immunoblotted with rabbit anti-FPPS antibody or rabbit anti-ERp57 antibody as a control.

(B) RNAi knockdown of FPPS inhibits influenza A/WSN replication. HeLa Tet-on cells were transfected with control or FPPS siRNA oligonucleotides as described in (A) and infected with influenza A/WSN virus at 24 hr after the second transfection. Viral titers in the supernatant were determined by plaque assay.

(C) RNAi knockdown of FPPS inhibits influenza A virus release. HeLa Tet-on cells were transfected as in (B). Ten hours after the second siRNA transfection, cells were infected with influenza A/WSN virus at an moi of 3. After 14 hr, the cells were pulse labeled, virus was released into the supernatant, and cellular viral proteins were immunoprecipitated at 3, 4, and 6 hr postchase and subjected to SDS-PAGE as described in Figure 2B.

DISCUSSION

Among the hundreds of interferon-inducible proteins, there are only a few for which an antiviral mechanism has been defined. Induction of PKR and 2′5′-OAS leads to an inhibition of protein synthesis and therefore prevents viral replication (Clemens and Elia, 1997; Kerr and Brown, 1978). ISG15 blocks ubiquitination of viral and cellular proteins important for HIV release (Okumura et al., 2006). Our data demonstrate that viperin inhibits the release of influenza virus at the final step in the viral life cycle, the release of the budding virus from the plasma membrane. This is a consequence of viperin-induced disruption of lipid-raft microdomains, and the data suggest that this results from an interaction of viperin with the enzyme FPPS that inhibits FPPS activity. Inhibition of the release stage of the viral replication cycle by disrupting lipid rafts has not previously been identified as a target of an interferon-inducible protein.

Lipid rafts play an important role in the replication cycle of many viruses. The envelopes of both influenza virus and HIV are enriched in raft lipids (Scheiffele et al., 1999; Brugger et al., 2006), and the budding process is initiated by the accumulation of viral envelope proteins in lipid rafts. Viperin expression reduced the extraction of lipid raft-associated HA by Triton X-100, commonly used to evaluate the association of membrane proteins with rafts, and also reduced copatching of the raft-associated sphingolipid GM1 with PLAP, a raft-associated protein, and, more importantly, with HA itself. FRAP analysis further showed that the lateral mobility of HA in the plasma membrane of viperin-expressing cells was increased, while the lateral mobility of the non-raft-associated transmembrane glycoproteins VSV-G was unaffected. In agreement with the hypothesis that these changes are directly responsible for the inhibitory effect of viperin, replication of VSV, which

does not bud from rafts, was unaffected by viperin expression. Viperin expression was recently shown to partially inhibit single-cycle VSV-pseudotyped HIV viral replication (Rivieccio et al., 2006), and it will be interesting to determine whether perturbation of lipid rafts by viperin also plays a role in controlling HIV infection.

The enzyme FPPS is a key player in the antiviral mechanism. Viperin binds to FPPS intracellularly and inhibits the activity of the enzyme. Although viperin is localized at the ER, we have shown that it resides at the cytoplasmic face, which is consistent with such an interaction (unpublished data). Inhibiting FPPS expression by siRNA affected influenza virus replication in a similar manner to viperin, namely by blocking viral release. Moreover, overexpression of FPPS in viperin-expressing cells reversed the increased fluidity of the plasma membrane and rescued influenza viral replication and release. We have attempted to determine which of the pathways downstream of FPPS is the key for the viperin-mediated effect. To date, the complexity of the FPPS pathway has rendered this ultimate goal elusive, but one can envision a number of possible mechanisms. Many cellular GTPases, such as members of the Ras family, are involved in intracellular vesicular transport, and many if not all are isoprenylated (Hancock et al., 1989). Isoprenoids such as farnesyl and geranylgeranyl lipids require FPPS for their synthesis, but we were unable to demonstrate an effect of viperin expression on the isoprenylation of candidate proteins. The fact that in vitro addition of cholesterol could partially restore normal fluidity in viperin-expressing cells suggested that cholesterol depletion could play a role. However, we have been unable to detect significant differences in the absolute levels of cholesterol or the rates of cholesterol biosynthesis between viperin-expressing and nonexpressing cells (data not shown). Nevertheless, the data clearly support a role for FPPS inhibition in the mechanism of action of viperin, and the observation that reducing FPPS levels by siRNA oligonucleotides affects influenza virus replication by perturbing membrane fluidity suggests a new therapeutic approach to controlling influenza virus infection.

EXPERIMENTAL PROCEDURES

Viruses, Cells, and Antibodies

Influenza A/WSN and A/PR8 viruses were kindly provided by Dr. Adolfo Garcia-Sastre. HeLa Tet-on cells were from Clontech. RAW261.4 cells were from ATCC. Goat anti-influenza antiserum was purchased from Chemicon. Rabbit antiserum to FPPS was kindly provided by Dr. Peter Edwards. The anti-HA mAb H17-L2 was kindly provided by Dr. Jonathan Yewdell. Goat anti-PGAM1 antiserum was from Abcam. Monoclonal Abs to GAPDH and GRP 94 were from Research Diagnostics. The anti-viperin mAb MaP.VIP was generated against the C-terminal domain of mouse viperin (amino acids 92–362).

Plasmids and Transfections

Mouse viperin was amplified from LPS-treated mouse primary macrophage cDNA and cloned into pCDNA3.1 vector between EcoRI and BamHI sites using the following primers: 5′-GGCCGAATTCAGGTG TGTGCCTATCACCATG-3′ and 5′-GCGCGGATCCATCTCAGCCTCA CCAGTCCA-3′. FPPS was amplified from NIH 3T3 cells cDNA and cloned between the same restriction sites using primers 5′-GCGCGAA TTCGCCATGAATGGGAACCAGAAA-3′ and 5′-GCGCGGATCCCTTT CTCCGTTTGTAGATCTT-3′. For some experiments, plasmids were transfected into HeLa Tet-on cells using Lipofectamine 2000 (Invitrogen) according to the manufacturer's recommendations. Transfection efficiencies were routinely determined by immunofluorescence and were minimally 85%.

HeLa Tet-on Viperin-Inducible Cells

Mouse viperin cDNA was subcloned into the pTRE-tight vector (Clontech). HeLa Tet-on cells were cotransfected with pTRE-tight viperin and a hygromycin resistance gene (Clontech). Positive clones were selected in the presence of G418 and hygromycin, and the inducibility of viperin was then determined by western blot analysis using a rabbit antiserum to viperin.

Immunofluorescence

Doxycycline-treated HeLa Tet-on viperin-inducible cells were fixed with 3.75% formaldehyde, permeabilized with 0.05% saponin, and stained with MaP.VIP and rabbit antibody to calnexin, followed by Alexa Fluor 546-conjugated goat anti-rabbit and Alexa Fluor 488-conjugated goat anti-mouse antisera (Molecular Probes). Images were acquired with a Leica TCS SP2 confocal microscope.

Radiolabeling and Immunoprecipitation

To examine the release of influenza A/WSN virus in the supernatant and viral proteins remaining in the cytosol, untreated or doxycycline-treated HeLa Tet-on viperin-inducible cells, or transfected HeLa Tet-on cells, were first infected with influenza A/WSN virus, deprived of methionine and cysteine for 30 min, pulse-labeled with ^{35}S-methionine and cysteine for 20 min, and chased for the noted intervals. Triton X-100 was added to the supernatants to a final concentration of 0.5%. Cells were lysed in Tris-buffered saline (pH 7.4) containing 1% Triton X-100. Immunoprecipitations were performed using 5 μl goat anti-influenza antiserum (Chemicon) and protein G Sepharose (Amersham), followed by SDS-PAGE.

Electron Microscopy

Thin-section electron microscopy was performed as previously described (Barman et al., 2003). Briefly, HeLa Tet-on vector or viperin-inducible cells were either untreated or treated with doxycycline for 24 hr and infected with A/WSN virus for 14 hr. Cells were fixed with 2.5% glutaraldehyde and postfixed with 1% osmiun tetroxide. Cells were en bloc stained with 2% uranyl acetate, dehydrated, infiltrated, and embedded in Epon. Sixty nanometer sections were stained with lead citrate and examined using a Tecnai 12 Biotwin electron microscope.

Antibody- and Cholera Toxin-Induced Patching

The copatching experiment was performed as described (Harder et al., 1998). Mouse anti-PLAP monoclonal antibody (NOVUS Biological) and mouse anti-HA monoclonal antibody H17-L2 were diluted 1:100, and Alexa 488-conjugated cholera toxin B subunit (Invitrogen, Molecular Probes) was used at 8 μg/ml. Cells were first washed in ice-cold PBS and then incubated with either PLAP or HA antibody and fluorescent cholera toxin B subunit at room temperature for 30 min. Cells were then washed briefly with ice-cold PBS and further incubated with Alexa 633 conjugated goat anti-mouse antibody for 30 min at room temperature. After washing with cold PBS, cells were fixed for 4 min in 3.7% formaldehyde at 4°C and subsequently incubated with methonal at −20°C for 5 min. Mounted cells were visualized, and images were acquired with a Leica TCS SP2 confocal microscope. For better visualization, Alexa 633 images were pseudocolored red using the Image J program.

Membrane Fluorescence Anisotropy Measurements

Membrane fluidity was determined by measuring fluorescence anisotropy in viperin-expressing cells and nonexpressing cells, using 1,6-diphenyl-1,3,5-hexatriene (DPH) (Sigma) as a probe. Cells were

incubated at 37°C for 5 min in Hank's balanced salt buffer (GIBCO) with DPH (4 mM). After washing the samples, fluorescence was measured at excitation wavelength 375 nm and emission wavelength 425 nm using a spectrofluorimeter (Photon Technology International). The anisotropy value was calculated as $r = (I_{VV} - G.I_{VH})/(I_{VV} + 2G.I_{VH})$ with $G = I_{HV}/I_{HH}$, $I_{HH} = I_{(L)HH} - I_{(buffer + cell)HH} - I_{(buffer + probe)HH} + I_{(buffer)HH}$ [$I_{(L)}$, fluorescence intensity of DPH probe-labeled cell suspension; $I_{(buffer + cell)}$, fluorescence intensity of nonlabeled cell suspension; $I_{(buffer + probe)}$, fluorescence intensity of buffer incubated with the DPH probe; $I_{(buffer)}$, fluorescence intensity of buffer alone].

FRAP Analysis

HeLa Tet-on RFP-inducible cells, either untreated or treated with doxycycline for 24 hr, were infected with influenza A/WSN virus for 14 hr. Cells were stained with Alexa 488-conjugated H17-L2 Fab on ice. FRAP analyses were conducted using a Leica TCS SP2 confocal microscope. Ten frames were collected at 0.834 s/frame before a 5 × 2 μm^2 area was photobleached at 40% laser power for 0.834 s. Fluorescence recovery was monitored by capturing confocal images at 3% laser power for 100 frames.

Yeast Two-Hybrid Screening

The Matchmaker GAL4 yeast two-hybrid system and a mouse embryonic fibroblast cDNA library (Clontech) were used. Mouse viperin cDNA was cloned into the pGBKT7 vector, and experiments were carried out following the manufacturer's instructions.

FPPS Activity Assay

FPPS activity was assayed as described (Reilly et al., 2002). Untreated and doxycycline-treated viperin-inducible cells were scraped into FPPS assay buffer. Lysates were cleared by centrifugation at 16,000 g for 10 min. Reactions were carried out in assay buffer containing 18 μM geranyl pyrophosphate, 13.3 μM [1-^{14}C] isopentenyl pyrophosphate, and 10 μg cell lysate protein at 37°C for 45 min. Samples were acidified, incubated in the presence of unlabeled farnesol at 37°C for 30 min to hydrolyze the FPP to farnesol, and then neutralized with 10% NaOH. Farnesol was extracted into hexane, and the organic phase was removed for liquid-scintillation counting.

Triton X-114 Partitioning

HeLa Tet-on vector cells or HeLa Tet-on viperin-inducible cells were either untreated or treated with doxycycline or lovastatin (5 μM) for 24 hr. Similarly to previously described methods (Overmeyer and Maltese, 1992), cells were lysed in 1% Triton X-114 in TBS with protein inhibitor cocktail on ice. Insoluble material was pelleted at 13,000 rpm for 10 min. Soluble factions were incubated at 37°C to promote phase separation, and the detergent phase was separated from the aqueous phase by centrifuging at 13,000 rpm for 1 min. The aqueous phase was removed and brought to 1% Triton X-114 by adding a 10% solution, and the concentration in the detergent phase was reduced to 1% by adding TBS. Protein concentration was then determined by the Bradford method, and equal amounts of protein were subjected to western blot analysis using antibodies specific for Cdc42, Rab5, and RhoB.

siRNA Transfection

Control and FPPS-specific siRNAs were obtained from Dharmacon. Briefly, 1 × 10^5 HeLa Tet-on cells were plated in 12-well tissue culture plates. Five microliters of 20 μM siRNA oligos was diluted to 100 μl, and 2 μl oligofectamine (Invitrogen) was used for each transfection following the manufacturer's recommendations. Twenty-four hours post-transfection, the cells were replated in one well of a 6-well plate to obtain 50% confluence the next day. Cells were transfected again with 10 μl of 20 μM siRNA oligos. Knockdown efficiency of FPPS was determined by western blot analysis.

Supplemental Data

The Supplemental Data include five supplemental figures and one supplemental movie and can be found with this article online at http://www.cellhostandmicrobe.com/cgi/content/full/2/2/96/DC1/.

ACKNOWLEDGMENTS

We thank Dr. Adolfo García-Sastre (Mount Sinai School of Medicine) for advice and for providing viruses and antibodies. We thank Dr. Peter Edwards (University of California, Los Angeles) for FPPS antibody and Dr. Jonathan Yewdell (National Institutes of Health) for H17-L2 antibody. We thank Drs. Michael Edidin, Samme Raza Shaikh, and Fang Yi for advice and assistance with membrane anisotropy analysis. We thank Dr. Derek Toomre for providing the VSV-G-GFP construct. We are indebted to Dr. Ming O. Li for critically reading the manuscript, constant advice, and assistance. We thank Dr. Marc Pypaert for EM work, Mary Pan for generating the viperin-specific monoclonal antibody, and Dr. David Stepensky for valuable assistance and advice with FRAP analysis. We also thank Dr. D. Peaper, Dr. K. Taraszka, and N. Joshi for discussions and Nancy Dometios for manuscript preparation. The work was supported by the Howard Hughes Medical Institute and the Ellison Medical Foundation. X.W. is supported by a Cancer Research Institute Postdoctoral Fellowship.

Received: March 19, 2007
Revised: May 16, 2007
Accepted: June 12, 2007
Published: August 15, 2007

REFERENCES

Almeida, P.F., Vaz, W.L., and Thompson, T.E. (1993). Percolation and diffusion in three-component lipid bilayers: Effect of cholesterol on an equimolar mixture of two phosphatidylcholines. Biophys. J. *64*, 399–412.

Arnon, T.I., Lev, M., Katz, G., Chernobrov, Y., Porgador, A., and Mandelboim, O. (2001). Recognition of viral hemagglutinins by NKp44 but not by NKp30. Eur. J. Immunol. *31*, 2680–2689.

Balint, E., Grimley, P.M., Gan, Y., Zoon, K.C., and Aszalos, A. (2005). Plasma membrane biophysical properties linked to the antiproliferative effect of interferon-alpha. Acta Microbiol. Immunol. Hung. *52*, 407–432.

Barman, S., Adhikary, L., Kawaoka, Y., and Nayak, D.P. (2003). Influenza A virus hemagglutinin containing basolateral localization signal does not alter the apical budding of a recombinant influenza A virus in polarized MDCK cells. Virology *305*, 138–152.

Barman, S., Adhikary, L., Chakrabarti, A.K., Bernas, C., Kawaoka, Y., and Nayak, D.P. (2004). Role of transmembrane domain and cytoplasmic tail amino acid sequences of influenza a virus neuraminidase in raft association and virus budding. J. Virol. *78*, 5258–5269.

Boudinot, P., Riffault, S., Salhi, S., Carrat, C., Sedlik, C., Mahmoudi, N., Charley, B., and Benmansour, A. (2000). Vesicular stomatitis virus and pseudorabies virus induce a vig1/cig5 homologue in mouse dendritic cells via different pathways. J. Gen. Virol. *81*, 2675–2682.

Brugger, B., Glass, B., Haberkant, P., Leibrecht, I., Wieland, F.T., and Krausslich, H.G. (2006). The HIV lipidome: A raft with an unusual composition. Proc. Natl. Acad. Sci. USA *103*, 2641–2646.

Chin, K.C., and Cresswell, P. (2001). Viperin (cig5), an IFN-inducible antiviral protein directly induced by human cytomegalovirus. Proc. Natl. Acad. Sci. USA *98*, 15125–15130.

Clemens, M.J., and Elia, A. (1997). The double-stranded RNA-dependent protein kinase PKR: Structure and function. J. Interferon Cytokine Res. *17*, 503–524.

Garrus, J.E., von Schwedler, U.K., Pornillos, O.W., Morham, S.G., Zavitz, K.H., Wang, H.E., Wettstein, D.A., Stray, K.M., Cote, M.,

Rich, R.L., et al. (2001). Tsg101 and the vacuolar protein sorting pathway are essential for HIV-1 budding. Cell *107*, 55–65.

Grewal, T.S., Genever, P.G., Brabbs, A.C., Birch, M., and Skerry, T.M. (2000). Best5: A novel interferon-inducible gene expressed during bone formation. FASEB J. *14*, 523–531.

Hancock, J.F., Magee, A.I., Childs, J.E., and Marshall, C.J. (1989). All ras proteins are polyisoprenylated but only some are palmitoylated. Cell *57*, 1167–1177.

Harder, T., Scheiffele, P., Verkade, P., and Simons, K. (1998). Lipid domain structure of the plasma membrane revealed by patching of membrane components. J. Cell Biol. *141*, 929–942.

Helbig, K.J., Lau, D.T., Semendric, L., Harley, H.A., and Beard, M.R. (2005). Analysis of ISG expression in chronic hepatitis C identifies viperin as a potential antiviral effector. Hepatology *42*, 702–710.

Kerr, I.M., and Brown, R.E. (1978). pppA2′p5′A2′p5′A: An inhibitor of protein synthesis synthesized with an enzyme fraction from interferon-treated cells. Proc. Natl. Acad. Sci. USA *75*, 256–260.

Khaiboullina, S.F., Rizvanov, A.A., Holbrook, M.R., and St Jeor, S. (2005). Yellow fever virus strains Asibi and 17D–204 infect human umbilical cord endothelial cells and induce novel changes in gene expression. Virology *342*, 167–176.

Kochs, G., and Haller, O. (1999a). GTP-bound human MxA protein interacts with the nucleocapsids of Thogoto virus (Orthomyxoviridae). J. Biol. Chem. *274*, 4370–4376.

Kochs, G., and Haller, O. (1999b). Interferon-induced human MxA GTPase blocks nuclear import of Thogoto virus nucleocapsids. Proc. Natl. Acad. Sci. USA *96*, 2082–2086.

Lamb, R.A., and Krug, R.M. (2001). Fields Virology, Volume 1 (Philadephia: Lippincott Williams & Wilkins).

Leser, G.P., and Lamb, R.A. (2005). Influenza virus assembly and budding in raft-derived microdomains: A quantitative analysis of the surface distribution of HA, NA and M2 proteins. Virology *342*, 215–227.

McCown, M.F., and Pekosz, A. (2006). Distinct domains of the influenza a virus M2 protein cytoplasmic tail mediate binding to the M1 protein and facilitate infectious virus production. J. Virol. *80*, 8178–8189.

Nathan, I., Ben-Valid, I., Henzel, R., Masalha, H., Baram, S.N., Dvilansky, A., and Parola, A.H. (1998). Alterations in membrane lipid dynamics of leukemic cells undergoing growth arrest and differentiation: Dependency on the inducing agent. Exp. Cell Res. *239*, 442–446.

Okumura, A., Lu, G., Pitha-Rowe, I., and Pitha, P.M. (2006). Innate antiviral response targets HIV-1 release by the induction of ubiquitin-like protein ISG15. Proc. Natl. Acad. Sci. USA *103*, 1440–1445.

Overmeyer, J.H., and Maltese, W.A. (1992). Isoprenoid requirement for intracellular transport and processing of murine leukemia virus envelope protein. J. Biol. Chem. *267*, 22686–22692.

Player, M.R., and Torrence, P.F. (1998). The 2-5A system: Modulation of viral and cellular processes through acceleration of RNA degradation. Pharmacol. Ther. *78*, 55–113.

Reilly, J.F., Martinez, S.D., Mickey, G., and Maher, P.A. (2002). A novel role for farnesyl pyrophosphate synthase in fibroblast growth factor-mediated signal transduction. Biochem. J. *366*, 501–510.

Rivieccio, M.A., Suh, H.S., Zhao, Y., Zhao, M.L., Chin, K.C., Lee, S.C., and Brosnan, C.F. (2006). TLR3 ligation activates an antiviral response in human fetal astrocytes: A role for viperin/cig5. J. Immunol. *177*, 4735–4741.

Samuel, C.E. (2001). Antiviral actions of interferons. Clin. Microbiol. Rev. *14*, 778–809.

Scheiffele, P., Roth, M.G., and Simons, K. (1997). Interaction of influenza virus haemagglutinin with sphingolipid-cholesterol membrane domains via its transmembrane domain. EMBO J. *16*, 5501–5508.

Scheiffele, P., Rietveld, A., Wilk, T., and Simons, K. (1999). Influenza viruses select ordered lipid domains during budding from the plasma membrane. J. Biol. Chem. *274*, 2038–2044.

Shvartsman, D.E., Kotler, M., Tall, R.D., Roth, M.G., and Henis, Y.I. (2003). Differently anchored influenza hemagglutinin mutants display distinct interaction dynamics with mutual rafts. J. Cell Biol. *163*, 879–888.

Sun, B.J., and Nie, P. (2004). Molecular cloning of the viperin gene and its promoter region from the mandarin fish Siniperca chuatsi. Vet. Immunol. Immunopathol. *101*, 161–170.

Szkopinska, A., and Plochocka, D. (2005). Farnesyl diphosphate synthase; regulation of product specificity. Acta Biochim. Pol. *52*, 45–55.

Zhu, H., Cong, J.P., and Shenk, T. (1997). Use of differential display analysis to assess the effect of human cytomegalovirus infection on the accumulation of cellular RNAs: Induction of interferon-responsive RNAs. Proc. Natl. Acad. Sci. USA *94*, 13985–13990.